

Polyethylene mixed crystal infra-red spectroscopy: The influence of matrix isotopic species on guest conformation

Stephen J. Spells

*H. H. Wills Physics Laboratory, University of Bristol, Tyndall Avenue,
Bristol BS8 1TL, UK*

(Received 10 May 1985)

The chain conformation of solution-crystallized polyethylene has previously been confirmed by infra-red spectroscopy, using the CD_2 bending bandshape for samples with a minority of the deuterated species¹⁻³. The method of calculating the i.r. band profile from molecular conformational models is now developed to give a more accurate representation of doublet splittings and to include the singlet component. The CH_2 bending profile is calculated for samples with a deuterated matrix, and the good agreement with experimental data indicates that the same molecular model is applicable for samples with the deuterated polymer as either guest or matrix, for identical crystallization conditions. This result implies that isotopic fractionation is unimportant under these conditions.

(Keywords: solution growth; polyethylene; mixed crystals; infra-red; chain conformation; isotopic fractionation)

INTRODUCTION

Isotopically labelled crystals of polyethylene have previously been used to establish the conformation of the individual polymer molecule¹⁻³. Two techniques, infra-red (i.r.) spectroscopy and neutron scattering, were used to obtain a detailed conformational model^{2,3} which is reviewed below. However, the i.r. technique was restricted in its quantitative application to samples where the 'guest' species was the fully deuterated polymer (PED) and the 'host' was normal polyethylene (PEH). In this work, we extend the technique to the reverse situation, where the normal 'guest' is dispersed in a deuterated matrix.

The model for crystals grown from xylene solution at 70°C is shown schematically in *Figure 1*. Several features are apparent. Firstly the crystal stems are arranged along sheets in the $\{110\}$ direction. These stems do not show perfect adjacent re-entry; the fold plane is diluted with other molecule(s) to the extent that 50% of the lattice sites along the $\{110\}$ direction are occupied by stems from a labelled molecule. There is an occasional fold in a different direction, giving rise to another sheet of stems. The resulting conformation involves several parallel sheets of stems (four in the case of *Figure 1*). The number of sheets increases with the guest molecular weight, with a molecular weight per sheet of 21 000. The figure of 75% for the probability of adjacent re-entry produces small groups of adjacent stems along the fold plane. Splittings in i.r. bending vibrations for the guest molecule result primarily from interactions between one labelled crystal stem and its nearest neighbours in $\{110\}$ directions. The magnitude of the splitting is related to both the size and shape of the group of adjacent stems, so that the conformation shown in projection at the top of *Figure 1* will produce several different doublet splittings. The distribution of these splittings is clearly dependent on the details of the specific molecular model used. This provides a method of checking whether the same conformation is present in samples with either PEH or PED matrix.

This extension of the i.r. technique is important, since both i.r. and neutron scattering methods rely on the fact that the different species generally behave identically; they are assumed only to differ significantly in monomer mass (and hence vibrational frequencies) and in the neutron scattering cross-section of the isotope. It is implicit that the two species crystallize in the same way, giving rise to the same statistical arrangement of crystal stems. However, there is known to be a melting point difference between PED and PEH, which may give rise to isotopic fractionation because of the different crystallization rates⁴. Previous i.r. and neutron scattering studies have deliberately focussed on rapid crystallization conditions, in order to minimize fractionation effects. Krimm and Ching have argued that these effects are unimportant in their i.r. samples, using PEH matrix⁵. For the alkane system $n\text{C}_{36}\text{H}_{74}/n\text{C}_{36}\text{D}_{74}$, they have shown the variation in isotopic composition of crystals formed from benzene solution with the degree of conversion for various initial isotopic compositions. The heterogeneity of crystals formed from equilibrium crystallization is greater for similar proportions of $\text{C}_{36}\text{H}_{74}$ and $\text{C}_{36}\text{D}_{74}$. Of particular significance here is the finding that the range of guest species concentrations within the crystal population is greater for a minority of $\text{C}_{36}\text{D}_{74}$. This dependence on the guest isotopic species is a result of their difference in melting points, which leads to the first crystals formed always being rich in $\text{C}_{36}\text{H}_{74}$. Any significant fractionation in polyethylene mixtures would also be expected to result in the hydrogenated species crystallising first. The concentration range of the guest species would depend on the guest isotope, with differences of chain conformation in the two cases. For neutron scattering measurements, we have previously shown that solution-grown samples with either PEH or PED matrices can be represented by the same molecular model¹. We attempt here to show whether the same conclusion can be drawn from i.r. studies, since measurements on samples with PED matrix have not previously been made with the benefit of recent

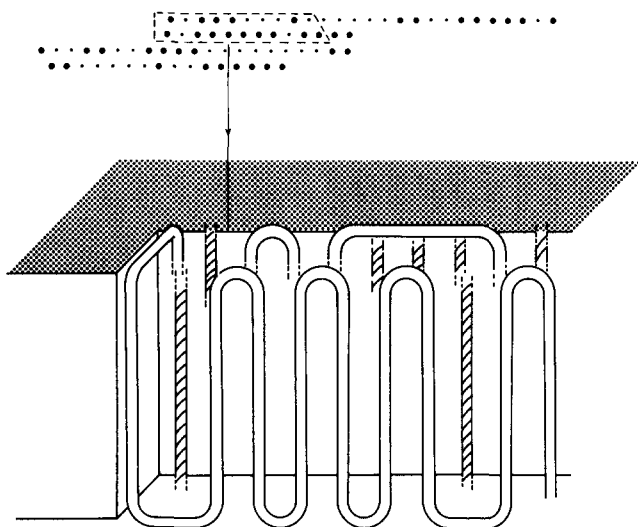


Figure 1 Schematic representation of the molecular conformation of a labelled polyethylene chain within the lamella. The large spots in the crystal stem projection at the top correspond to the unshaded molecule in the perspective sketch. The $\{110\}$ direction is horizontal

developments in instrumentation and analysis. If significant fractionation occurs under the crystallization conditions adopted (from dilute xylene solution at 70°C), a different molecular model would be required to fit the neutron scattering and i.r. data for the two systems. On the other hand, if one molecular model proves adequate for both sample types, then fractionation must be unimportant.

The use of Fourier Transform i.r. (FTi.r.) spectroscopy with samples cooled to liquid nitrogen temperatures has improved the quality of mixed crystal spectra, and we have recently shown that the spectral resolution can be further improved by Fourier self-deconvolution³. This technique has confirmed the presence of a large number of doublet components within the bending vibrational profile, and the splittings and relative intensities compare favourably with calculations using our statistical model. In the present work, we make several advances in the calculation of i.r. spectra and in the data analysis. The CX_2 ($\text{X} = \text{H}$ or D) bending vibration appears generally as a superposition of various doublet components and a central singlet. This latter peak was omitted in our earlier calculations^{2,3}, but here we use the measured sample crystallinity, together with information from our molecular models, to include the singlet in our calculations. Secondly, we have previously assumed that all doublets show the same frequency for the low frequency components^{2,3}. Here we utilise the deconvoluted spectra to establish the shift in frequencies with doublet splitting, which is then incorporated in our models. These two modifications to the calculation of spectra greatly improve their quality, and allow a more detailed comparison between calculation and experiment. Finally, we have introduced a single parameter to characterize any spectrum, calculated or experimental. This is the second moment of the band profile about the central singlet. Each doublet consists of one component of higher frequency than the singlet and another of lower frequency. Since all the relevant information is contained to one side (high or low frequency) of the singlet, the moment is calculated over the high frequency side only. This provides a simple method of comparison between calculated and experimental data.

PED matrix doublet splittings

The mixed crystal i.r. technique was applied at an early stage to PED matrix samples as well as PEH matrix⁶. In solution-crystallized materials, the guest (X) species gave rise to a doublet in the CX_2 bending vibration for both types of sample, indicating the presence of adjacent stems along the $\{110\}$ direction. More recent low temperature measurements have shown that the band profiles are complex, with a number of doublet contributions^{2,3,7}. This, in itself, is evidence for the existence of several possible environments for guest stems. A more detailed analysis was clearly necessary.

The first stage was the use of coupled oscillator theory, with the repeating unit as the two non-equivalent stems in the unit cell (i.e. a pair of oscillators). Splittings were calculated for finite sheets of adjacent stems, and the method was extended to include multiple sheets⁷. Such structures had already been anticipated by the superfolded multiple-sheet model for solution-crystallized polyethylene⁸. To apply the coupled oscillator theory to these arrays of crystal stems, assumptions were made about the type of inter-stem coupling involved and the freedom of the boundaries for groups of adjacent stems⁷. Despite being only a semi-empirical treatment, this approach avoids the complexity of more rigorous normal mode calculations.

We have since extended this method to deal with the more irregular groups of adjacent stems which arise from the statistical model developed for solution-grown polyethylene crystals². The main features of the statistical model¹ will now be restated briefly. The molecular stems are arranged in sheets along the $\{110\}$ direction. A labelled molecule is diluted by 50% along the fold plane by other molecule(s), and there is a 75% probability of folding to the adjacent site. The one variable used to model labelled molecules with different molecular weights is the number of parallel sheets of stems, which is allowed to increase in proportion to \bar{M}_w .

For any statistical model, we can obtain a computer-generated set of molecular conformations. It is useful at this stage to repeat briefly the terminology introduced in ref. 2. The irregular arrangements of guest stems produced by the program can be divided into *groups* of labelled stems, in which each stem has a labelled nearest neighbour in a $\{110\}$ direction. Each group is then transformed into an *equivalent group*, which has a similar number of stems to the original group and a similar distribution of $\{110\}$ interactions. The sheets of stems start in register along a $\{110\}$ plane other than the fold plane and are not diluted with other molecules. However, there may be different numbers of stems in successive sheets. *Figure 2a* shows an example. An equivalent group with equal numbers of stems in all sheets is termed a *closed group*. Groups of this kind were analysed by Cheam and Krimm⁷, who calculated the splittings for different group dimensions. An example is shown in *Figure 2b*. For less regular arrangements of stems, it is still possible to define part of the equivalent group as closed. This part is called a *closed subgroup*. *Figure 2a* includes, in the terminology of ref. 2, a (3×2) closed subgroup. An equivalent group may include several alternative closed subgroups, and the subgroup with the maximum splitting (as calculated from coupled oscillator theory⁷) is used as the basis for calculating the doublet splitting for the equivalent group². Additional stems within the equivalent group, which are not included



Figure 2 (a) An (8,3) equivalent group and (b) an (8 × 3) closed group, both shown in projection with the {110} direction horizontal

in the closed subgroup, provide additional {110} interactions which increase the splitting.

The same methods can now be applied to PED matrix samples. We start by calculating the CH₂ bending mode splittings for closed groups of stems. A sheet of stems is considered as a series of oscillator pairs, arranged along a {110} plane. The splitting for N such pairs is then determined by two other splittings—that for a single oscillator pair and that for an infinite sheet. Using a pure PEH sample cooled with liquid nitrogen, the CH₂ bending doublet was found to have a splitting of 13.5 cm⁻¹. For a single infinite sheet, the number of interactions per stem is halved, leading to a splitting

$$\Delta v_{\infty} = \frac{13.5}{2} \text{ cm}^{-1} = 6.75 \text{ cm}^{-1}$$

A value of 2.62 cm⁻¹ has been deduced for the splitting from an isolated pair of PED stems⁷. Scaling this by the ratio of infinite sheet splittings for PEH and PED gives an isolated pair splitting (Δv_0) of 3.47 cm⁻¹ for PEH. (It is noteworthy that this value is within 0.1 cm⁻¹ of $\Delta v_{\infty}/2$. From the argument above, the two values are expected to be identical). With these values for Δv_{∞} and Δv_0 , we calculated splittings for single and multiple sheets in the same way as for CD₂ bending modes⁷. Splittings for the irregular groups generated by statistical models were then computed as in the earlier work².

Calculation of spectra

In the previous work, which concerned PEH matrix single crystals, a specific molecular model was used as the basis for all calculations². A computer-generated set of molecular conformations, including that shown in *Figure 1*, was analysed as outlined above, and the doublet splittings were calculated and their components summed. The low frequency components of all doublets were assumed to coincide in frequency, and the singlet contribution was omitted from the calculations. A Lorentzian lineshape was used to allow for line broadening. It was found that better agreement could be obtained using these computed spectra and experimental data if the measured spectra were first subjected to Fourier self-deconvolution³. The reason is probably the difficulty of estimating component bandwidths where the original components are poorly resolved. The deconvolution improves the spectral resolution, so that the correct choice of bandwidth for the corresponding computed spectra is easily made.

The self-deconvolution technique allows the frequencies of individual components to be determined to a high degree of accuracy. Under favourable conditions, one doublet may have a significantly higher intensity than any other, and the two components may be unambiguously identified. In this way, the frequencies of the two components can be assigned to a particular splitting. In order to obtain a range of doublet splittings, it was necessary to use both solution-crystallized samples (where the outer-

most doublet is generally the most intense) and similar samples subjected to heat annealing. The latter sample type has been studied in detail, and the analysis will be presented elsewhere⁹. It is sufficient here simply to note that, confining ourselves to the temperature range where lamellar thickening occurs, the maximum splitting initially decreases with temperature of annealing. A range of splittings is therefore available for the calibration of splitting as a function of doublet component frequencies. The results were plotted for both PEH and PED matrix samples. In the case of PEH matrix samples, both high and low frequency components could be fitted to straight lines, using a least squares procedure. The results were

$$v_{\text{high}} = 1087.4 + 0.64(\Delta v) \text{ cm}^{-1}$$

$$v_{\text{low}} = 1087.4 - 0.36(\Delta v) \text{ cm}^{-1}$$

where Δv is the doublet splitting corresponding to components at v_{high} and v_{low} . The singlet frequency had the constant value of 1087.8 cm⁻¹.

For the PED matrix samples, neither the high nor the low frequency components could be fitted to a single straight line, since plots of frequency versus splitting showed some curvature. An adequate fit was, however, obtained for each component using two straight lines. For splittings $\Delta v \leq 9.1 \text{ cm}^{-1}$, least squares fits produced the results:

$$v_{\text{high}} = 1466.1 + 0.73(\Delta v) \text{ cm}^{-1}$$

$$v_{\text{low}} = 1466.1 - 0.27(\Delta v) \text{ cm}^{-1}$$

and for $\Delta v > 9.1 \text{ cm}^{-1}$:

$$v_{\text{high}} = 1470.1 + 0.29(\Delta v) \text{ cm}^{-1}$$

$$v_{\text{low}} = 1470.1 - 0.71(\Delta v) \text{ cm}^{-1}$$

In this case the singlet frequency was 1466.7 cm⁻¹.

The reason for this difference between the behaviour for PEH and PED matrix materials is not clear; the component frequencies can be determined with similar accuracy in either case and the numbers of calibration points used were similar. The relationships quoted above nevertheless form an empirical basis for determining the frequency components corresponding to any calculated splitting.

In our earlier calculations of CD₂ bending profiles, the central singlet component was excluded^{2,3}. This component includes contributions from non-crystalline material, isolated labelled stems within the crystal lattice and rows of crystal stems with fold directions other than {110}. The major reason for omitting this band was the apparent sensitivity of frequency position to the type of fold arrangement⁷. However, the deconvoluted spectra presented in this work show no evidence of singlet components with different frequencies. The central peak shows a constant frequency, with no indication of shoulders attributable to other components, and the minimum doublet splittings observed show good agreement with the calculations for an isolated pair of non-equivalent stems. Furthermore, the molecular model which we have derived for solution grown crystals of polyethylene does not include any significant proportion of folding along directions other than {110}¹. Crystal stems which are isolated on {110} planes may have the occasional si-

ilarly isolated nearest neighbour in, for example, the {200} plane. The neighbouring stems would not then be connected by a fold. Because of their crystallographic relationship, their contribution to the CD₂ bending vibration would be a singlet. Our computer-generated molecular models can be searched for such sequences, along with isolated stems (i.e. stems with no nearest neighbours of the same isotopic species). In the calculations to follow, both contributions are taken to occur at the same (singlet) frequency.

To include the singlet contribution to the i.r. band profile, it is necessary to consider its intensity relative to the doublet components. Taking, for example, the CD₂ bending vibration for a sample with PEH matrix, the resultant dipole moment change for any CD₂ unit is in a direction bisecting the angle DCD. Consider now a row of neighbouring PED stems, arranged along the {110} plane. In any *ab* plane, the CD₂ units from successive stems show an alternation in the direction of the dipole moment change. The directions for all the CD₂ units within the group of neighbouring stems must be used to derive an overall direction of change for the group. However, two points are evident without the benefit of detailed calculations.

First, the intensity of a doublet is decreased, relative to a singlet, by the fact that dipole moment changes from neighbouring CD₂ units are not all parallel. The calculated doublet intensity should strictly be reduced to allow for this. However, we have already noted that there are various contributions to the singlet. Some of these arise from disordered chains and others from chains within oriented crystal lamellae. The proportions of these contributions are variable among different samples, as is the degree of orientation of the lamellae. For this reason, the singlet contribution has simply been scaled by the total number of units from the different structures. Nevertheless, we expect that the calculated singlet intensity will generally be somewhat less than for experimental data, the discrepancy depending on the detailed sample morphology.

The second point concerns the doublet components, and the way in which PED stems are arranged in our molecular model. They are distributed along parallel {110} crystal planes. If the two stem orientations within the unit cell are labelled A and B, then for any group of neighbouring PED stems there may be unequal numbers, n_A and n_B , of stems in the two orientations. Clearly, for a group confined to 1 sheet with an even number of stems ($n_A + n_B$), then $n_A = n_B$. For an odd number of stems, $|n_A - n_B| = 1$. For larger numbers of sheets, the situation can become more complex, and $|n_A - n_B|$ may exceed 1. In general, $|n_A - n_B|$ is likely to be small by comparison with $n_A + n_B$. The majority of the stems can therefore be 'paired' with neighbours of the different orientation and sharing the same fold plane. This means that the direction of the overall dipole moment change for a group of stems is insensitive to the size of the group. To a first approximation, we have assumed that the direction of the dipole moment change is the same for each group, so that no scaling of certain doublets relative to others is necessary.

For the purpose of the singlet intensity calculation, the proportion of non-crystalline chains was calculated from d.s.c. measurements of sample crystallinity. Representative crystallinities for PED and PEH matrix samples were 0.75 and 0.8 respectively. Non-crystalline chains

were assumed to give a singlet component with the same frequency as the other contributions, and all contributions were weighted in proportion to the numbers of monomer units involved.

In addition, there is a clear need for a single quantity to represent the intensity distribution within a CX₂ bending profile, either calculated or experimental. The outermost doublet generally has the maximum intensity for the crystals studied here, and its splitting is very sensitive to molecular weight for moderate values of molecular weight. We have therefore chosen a quantity which is sensitive to the largest splittings present, namely the second moment of the absorbance distribution. Taking the singlet frequency as the origin, similar information is contained within the band profile to either low or high frequency of this origin. Only the high frequency side of the distribution was used for our calculations. The second moment was therefore defined as

$$M_2 = \sum_{v=v_s}^{v_e} A_N(v)(v-v_s)^2$$

where $A_N(v)$ is the absorbance at frequency v , normalized over the interval from the singlet frequency v_s to the high frequency limit of the band profile, v_e . As noted earlier, it has been found that a comparison between calculated and experimental data is more satisfactory if the deconvoluted experimental spectrum is used, rather than the original data. The second moment was therefore calculated for deconvoluted data.

All spectra were recorded with samples cooled to liquid nitrogen temperatures in a Nicolet 7199 Fourier Transform Interferometer. The instrumental resolution was 1 cm⁻¹ and typically 500 scans were collected for each spectrum. Deconvolution was carried out as previously described³, using the Nicolet software. Typical values for the deconvolution parameters representing the Lorentzian natural linewidth and the resolution enhancement factor were 2.0 cm⁻¹ and 3.0 for PED matrix samples and 1.7 cm⁻¹ and 5.0 for PEH matrix. All samples were crystallized from dilute solution in xylene at 70°C and sedimented, dried and pressed before making i.r. measurements.

PEH matrix results

In Figures 3–6, we compare experimental data (bottom), the same data after deconvolution (middle) and calculated spectra (top). In each case the calculated curve corresponds to a set of computer-generated crystal stem models, each of which has been divided into groups of labelled stems. Each such group has then been used to derive an equivalent group, and the group doublet splitting was then calculated as in previous work^{2,3}. The i.r. spectrum was generated, using the relationships between splittings and frequencies quoted above. The singlet intensity was obtained by adding the contributions from isolated crystal stems and from non-crystalline material, the latter being assumed to constitute 20% of the material. All peaks were then broadened, using a Lorentzian broadening function of half-width 0.5 cm⁻¹.

In each case, the calculation shown is based on models with the (integer) number of sheets of crystal stems closest to $\bar{M}_w/21\,000$, where \bar{M}_w is the molecular weight measured for the appropriate sample. The figure of 21 000 was derived for the average molecular weight per sheet from

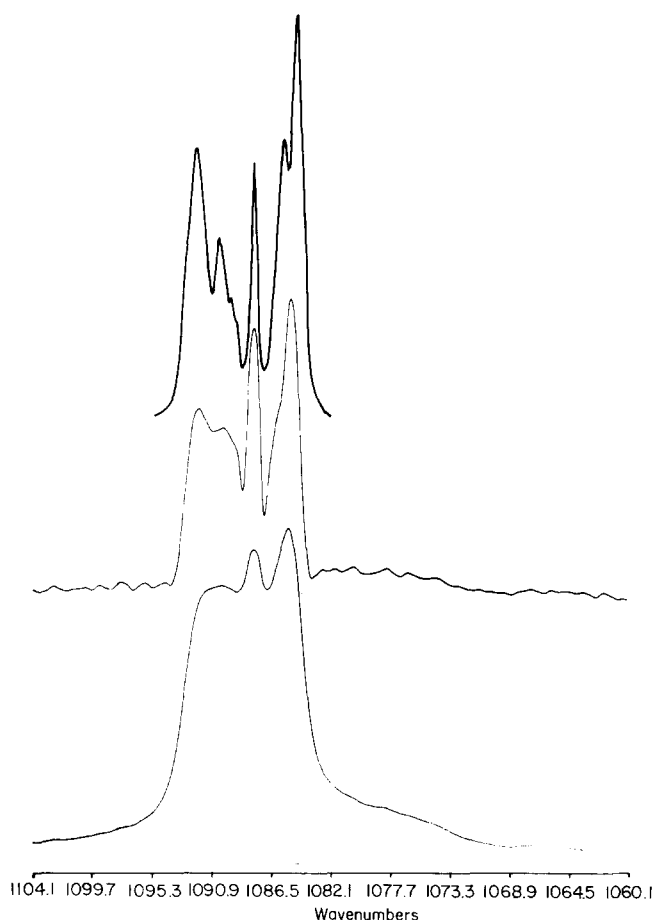


Figure 3 Bottom: experimental spectrum for sample with 3% PED of $M_w = 54\,000$ in PEH matrix. Middle: experimental spectrum after Fourier self-deconvolution. Top: calculated spectrum for the same model as shown in *Figure 1*, but with 3 parallel sheets of stems

fitting neutron scattering data to our molecular model¹. The only exceptions to this procedure are in *Figures 6* and *7*. The molecular weight of the sample illustrated in *Figure 6* ($M_w = 386\,000$) corresponds to 18 sheets. Both neutron scattering and infra-red techniques become insensitive to the number of sheets as the number increases^{1,2}: i.r. spectra for models with 4 and 11 sheets have, in particular, been shown to have remarkable similarities. This reflects the similar distribution of sizes of labelled stem groups, resulting from the re-entry statistics used in our model. A model with 11 sheets was therefore used in order to simplify the computation of the spectrum in *Figure 6*: any differences between models with 11 and 18 sheets will be negligible. The molecular weight of the sample in *Figure 7* corresponds to 10 sheets, and a comparison with the calculation for the 11 sheet model in *Figure 6* is adequate. The close similarity between the experimental data shown in *Figures 6* and *7* confirms that the i.r. spectrum is insensitive to the number of sheets for sufficiently high molecular weights.

The general agreement between deconvoluted experimental spectra and the calculated curves is seen to be good. The outermost doublet splitting (corresponding to the components with highest and lowest frequencies) is generally within 1 cm^{-1} for the two curves, the calculated values being consistently larger. The experimental outermost splittings range from 6.8 to 8.3 cm^{-1} . The positions of inner doublets are well reproduced, although

their intensities are generally higher in the computed spectra. The intensity of the central singlet (the well resolved peak at 1087.8 cm^{-1}), relative to the outermost doublet intensities, is in reasonable agreement for calculated and deconvoluted spectra, the agreement improving with increasing molecular weight. In general, however, the calculated singlet intensity is less than the experimental value, as predicted above. As another indication of the degree of agreement, values for the second moment of the intensity distributions are shown in *Table 1*. The value of the second moment is clearly dominated by the intense outermost doublet components, so that small differences in their splittings and intensities for experimental and calculated curves are emphasized in the moment. This is the chief reason for the higher values of the model moments than the experimental moments. By contrast, we can calculate the value of M_2 for another model proposed for polyethylene single crystals¹⁰. This model uses a lattice theory for the chain packing at interfaces. The proportion of adjacent re-entry, the major difference compared with our own model, is predicted to be less than 20%. We have previously calculated the i.r. spectrum for such a model, using 19% adjacent re-entry and 50% molecular dilution along the sheet³. It was shown that the outermost doublet splitting was considerably smaller than for our preferred model, which incorporates 75% adjacent re-entry. We calculate a value of 3.0 for M_2 , for a 3-sheet model with 20% adjacent re-entry and 50% dilution. This figure is clearly considerably

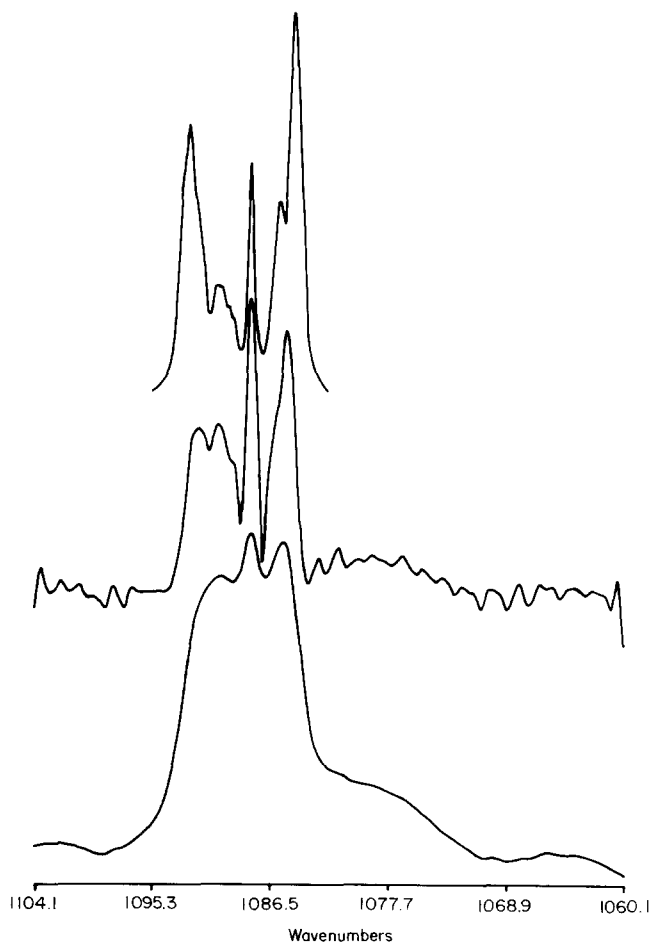


Figure 4 Bottom: experimental spectrum for 1% PED of $M_w = 93\,300$ in PEH matrix. Middle: deconvoluted spectrum. Top: calculated spectrum from model shown in *Figure 1* with four sheets

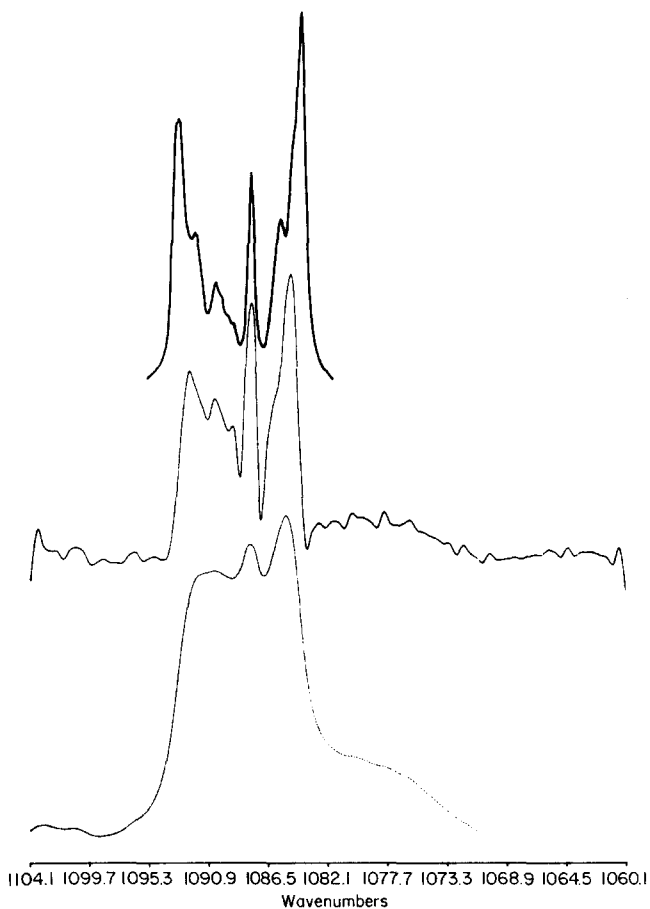


Figure 5 Bottom: experimental spectrum for 1% PED of $\bar{M}_w = 155\,400$ in PEH matrix. Middle: deconvoluted spectrum. Top: calculated spectrum for preferred model (Figure 1) with 7 sheets

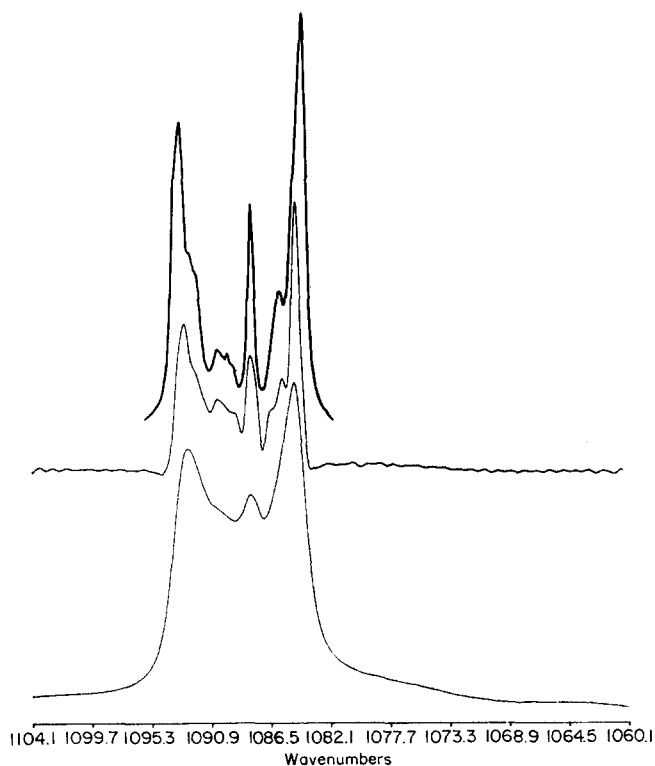


Figure 6 Bottom: experimental spectrum for 3% PED of $\bar{M}_w = 386\,000$ in PEH matrix. Middle: deconvoluted spectrum. Top: calculated spectrum for preferred model with 11 sheets

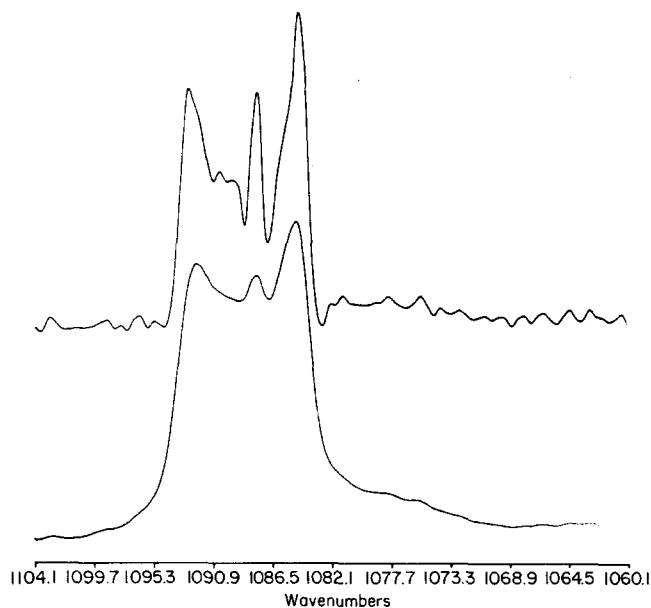


Figure 7 Bottom: experimental spectrum for 3% PED of $\bar{M}_w = 216\,000$ in PEH matrix. Top: deconvoluted spectrum

Table 1 Values for the second moment of the absorbance distribution about the singlet frequency for experimental and calculated PEH matrix i.r. spectra

PED molecular weight ^a $\bar{M}_w \times 10^{-3}$	Figure number (this work)	Second moment M_2 expt. (cm^{-2})	N_{sh}^b	Second moment M_2 model (cm^{-2})
54.0	3	8.0	3	11.2
93.3	4	7.6	4	13.2
155.4	5	9.1	7	15.6
216.0	7	11.3	11	17.3
386.0	6	12.6	11	17.3

^a Molecular weight determined by g.p.c.

^b Number of sheets used in molecular model

smaller than both the experimental value of 8.0 and the preferred model value of 11.2. Differences between other model and experimental values quoted in Table 1 are generally small by comparison, providing further evidence for the inadequacy of the lattice theory model.

PED matrix results

Figures 8–11 show experimental data, deconvoluted spectra and calculated spectra. The calculations were done in the same way as for PEH matrix samples, with the assumption of 25% non-crystalline material in this case. The experimental spectra show an additional peak at 1456 cm^{-1} , which has no equivalent in PEH matrix spectra. A band at 1442 cm^{-1} has been observed for cyclic paraffins, but not in their linear analogues¹¹. It was attributed to a CH_2 bending vibration of the tight fold conformation. It is possible that the 1456 cm^{-1} band has a similar origin. There may be coupling with the methyl group asymmetric bending mode, which usually appears at similar frequencies. The isotope frequency shift differs for the two vibrations, so that coupling may be prevented in PEH matrix samples, leading to the absence of a corresponding peak. Furthermore, the relatively large frequency difference between the 1456 cm^{-1} band and the multiplet structure at higher frequencies makes it appear unlikely that the 1456 cm^{-1} peak is associated with the multiplet structure.

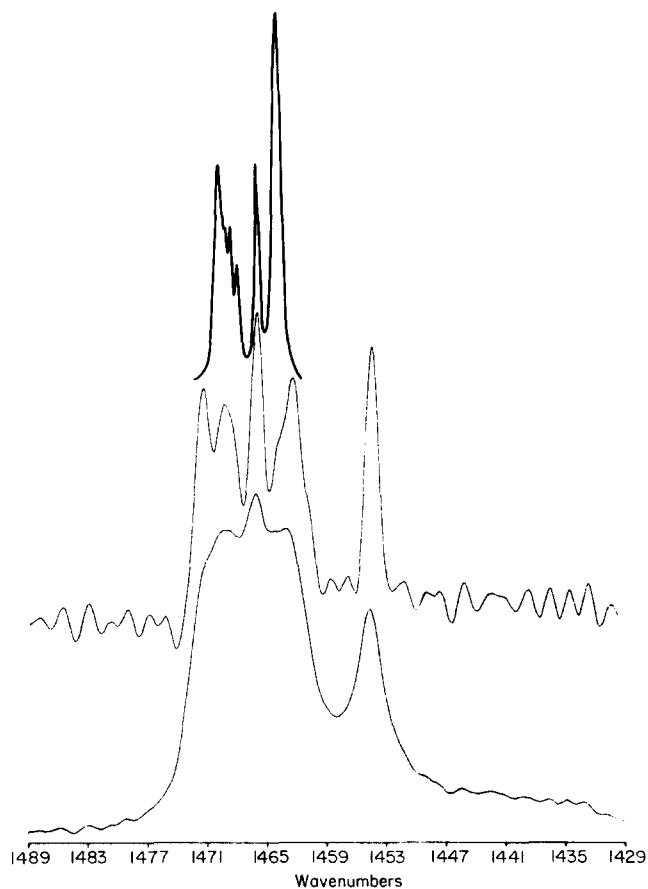


Figure 8 Bottom: experimental spectrum for 5% PEH of $\bar{M}_w = 15\,000$ in PED matrix. Middle: deconvoluted spectrum. Top: calculated spectrum for preferred model with 1 sheet

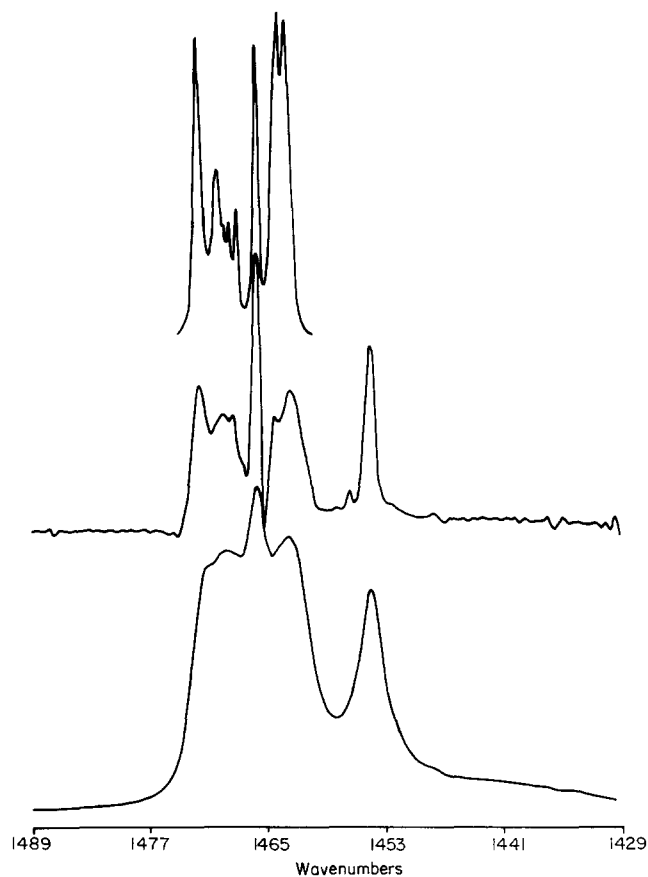


Figure 9 Bottom: experimental spectrum for 3% PEH of $\bar{M}_w = 28\,600$ in PED matrix. Middle: deconvoluted spectrum. Top: calculated spectrum for preferred model with 2 sheets

Table 2 Second moment values for PED matrix samples

PEH molecular weight $\bar{M}_w \times 10^{-3}$	Figure number (this work)	Second moment M_2 expt. (cm^{-2})	N_{sh}	Second moment M_2 model (cm^{-2})
15.0	8	16.1	1	8.9
28.6	9	14.4	2	17.3
51.0	10	16.2	2	17.3
87.0	11	22.6	4	22.9

In *Figure 8*, the calculated spectrum (top) corresponds to a calculation based on a molecule occupying 1 sheet of stems. The deconvoluted experimental spectrum (centre) shows a larger outermost splitting, and is better reproduced by a 2 sheet model (*Figure 9*, top). Experimental and calculated values of the second moment, M_2 , are listed in *Table 2*, and also show better agreement between the 2 sheet model and the experimental spectrum for the sample with $\bar{M}_w = 15\,000$. In fact, neutron scattering results for this sample also indicated best agreement with a calculation for more than one sheet of stems¹. The deconvoluted data for molecular weights of 28 600 (*Figure 9*) and 51 000 (*Figure 10*) are also in good agreement with the 2 sheet model, as regards the positions of doublet components and their relative intensities. This result is consistent with that from neutron scattering¹, which showed a small increase in the number of stems per sheet on increasing the molecular weight. However, the calculated singlet intensity in *Figure 9* is smaller than the

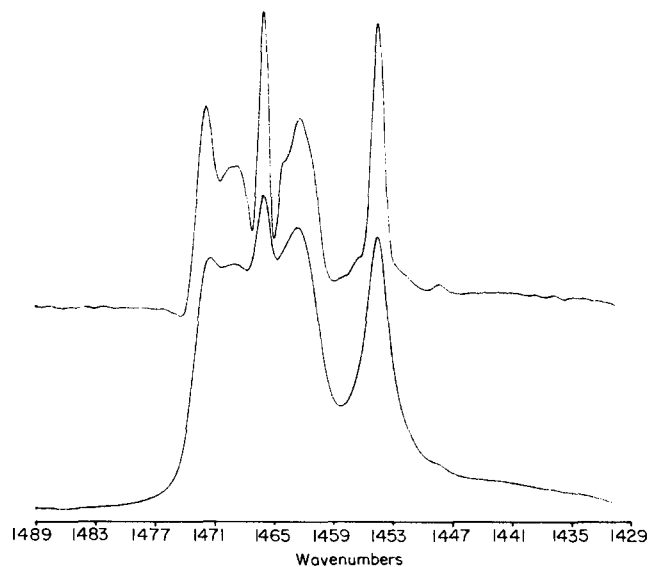


Figure 10 Bottom: experimental spectrum for 3% PEH of $\bar{M}_w = 51\,000$ in PED matrix. Top: deconvoluted spectrum

experimental values in *Figures 9* and *10*, by comparison with the doublet intensities, as was anticipated earlier. The same comments also apply to the highest molecular weight samples (*Figure 11*). Model and experimental values of M_2 are in closest agreement for the higher molecular weights (*Table 2*).

The overall agreement between observed and calculated spectra is therefore slightly better for PED matrix

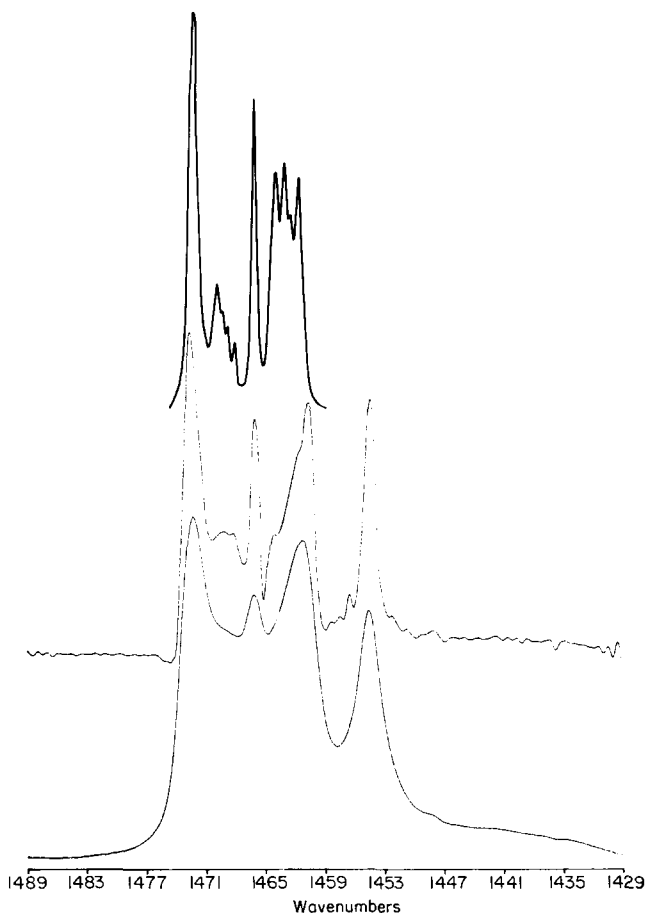


Figure 11 Bottom: experimental spectrum for 3% PEH of $\bar{M}_w = 87\,000$ in PED matrix. Middle: deconvoluted spectrum. Top: calculated spectrum for preferred model with 4 sheets

than for PEH matrix samples. In both cases, the agreement is good, and the i.r. results clearly provide further support for the molecular model used.

CONCLUSIONS

By extending the mixed crystal i.r. technique to samples crystallized in a PED matrix, and improving the method of calculating i.r. spectra, we have shown that our model for the chain conformation presented earlier¹ is applicable in general to samples crystallized from xylene solution at 70°C. This is important in demonstrating that isotopic fractionation is negligible under these conditions of crystallization.

It will be shown elsewhere⁹ that, under suitable conditions, isotopic fractionation *can* be detected with the i.r. method. Its absence in this case is further evidence that the model chain conformation is representative of molecules in the homopolymer.

ACKNOWLEDGEMENTS

Support for this work from the SERC is acknowledged. I wish to thank Professor A. Keller and Dr D. M. Sadler for their encouragement and advice. I am grateful to Mrs A. Halter for technical assistance.

REFERENCES

- 1 Spells, S. J. and Sadler, D. M. *Polymer* 1984, **25**, 739
- 2 Spells, S. J., Keller, A. and Sadler, D. M. *Polymer* 1984, **25**, 749
- 3 Spells, S. J. *Polymer* 1984, **25** (Commun.), 162
- 4 Stehling, F. S., Ergos, E. and Mandelkern, L. *Macromolecules* 1971, **4**, 672
- 5 Krimm, S. and Ching, J. H. C. *Macromolecules* 1972, **5**, 209
- 6 Bank, M. I. and Krimm, S. J. *Polym. Sci., A-2* 1969, **7**, 1785
- 7 Cheam, T. C. and Krimm, S. J. *Polym. Sci. Polym. Phys. Edn.* 1981, **19**, 423
- 8 Sadler, D. M. and Keller, A. *Science* 1979, **203**, 263
- 9 Spells, S. J. and Sadler, D. M., to be published
- 10 Yoon, D. Y. and Flory, P. J. *Macromolecules* 1984, **17**, 868
- 11 Grossman, H. P., Arnold, R. and Bürkle, K. R. *Polym. Bull.* 1980, **3**, 135